Environ Res Tec, Vol. 7, Issue. 4, pp. 578–587, December 2024

Environmental Research and Technology
https://ert.yildiz.edu.tr - https://dergipark.org.tr/tr/pub/ert
DOI: https://10.35208/ert.1425123

Research Article

Numerical analysis of transient soil temperature variation during wildfires

Mehmet Turgay PAMUK*

Department of Mechanical Engineering, Okan University Faculty of Engineering and Natural Sciences, İstanbul, Türkiye

ARTICLE INFO

Article history
Received: 24 January 2024
Revised: 30 May 2024
Accepted: 03 June 2024

Key words:
Conduction; Pipe lines; Radiation; Soil properties; Transient heat transfer; Wild fires

ABSTRACT

In this study, transient behavior of soil temperature during large forest fires is analyzed using the Comsol© software package. The increase in soil temperature during large wildfires can be very critical, especially when oil or gas pipelines have been laid at a certain depth in the soil mainly near forests. During forest fires, the temperature of the soil surface can reach extreme levels that penetrate deep into the ground if the fire is not extinguished within a short time. This increase in temperature on the soil surface can lead to extremely dangerous situations if the laying depth of the pipeline is not sufficient, as the heat conducted through the soil causes the surface temperature of the pipeline and therefore that of the fluid inside it to reach even high values. This can lead to a sudden rupture of the pipeline and ultimately lead to catastrophic consequences. The present study is conservative due to the assumptions made in structuring the numerical model. However, it is believed to provide invaluable information about the considerations in selecting gas pipeline locations and pipeline laying depths taking into account extreme temperatures due to wildfires. There is limited research on the topic regarding the time dependent conduction heat transfer through soils as a result of fires, but only in one dimension. Current study, being multi-dimensional, is therefore believed to be novel in the field. Future research could include extensive study on the energy content of different species of forest trees, considering their time-dependent heat release rates (HRR) during a forest fire, as well as experimental work if a field setup could be designed.

Cite this article as: Pamuk MT. Numerical analysis of transient soil temperature variation during wildfires. Environ Res Tec 2024;7(4)578–587.

INTRODUCTION

In recent decades, drastic climate changes have been observed due to global warming, caused primarily by ever-increasing concentrations of greenhouse gases and leading to unusual atmospheric phenomena such as extreme temperatures and drought [1]. These extreme temperatures coupled with low humidity pose a great risk of forest fires, especially in pine forests [2]. Once such fires start, they can spread over a large area in a short time and last for days until all the fuel (burning energy from living or dead biomass) is used up. As a result of these fires, dramatic consequences can occur such as loss of biodiversity as well as air pollution and deterioration of the physicochemical and biological properties of the soil. Currently, forecasting models based on fuel maps, remote sensing indices and statistical data can be used to predict the occurrence of wildfires [3]. A recent study evaluates the possibility of use of long time series, 30-m resolution fractional forest cover data obtained from satellites combined with multi-source data and integrated with multiple analysis methods [4]. Singh and Huang [5] used a machine learning approach to identify the role of climatic and anthropogenic factors in influencing fire probability and to map the spatial distribution of fire

***Corresponding author.**
*E-mail address: turgaypamuk@hotmail.com

risk over a two-decade period. Climate change is having a strong impact on natural wildfire activity worldwide. For instance, naturally caused wildfires in the western United States have increased throughout history, particularly the southwest region has the highest wildfire activity under historical conditions [6]. Similarly, compared to other states in the northwestern Himalayas, Uttarakhand is the state with the highest risk of forest fires among Indian states. It is also shown that fires occur more frequently in the month of May and that evergreen coniferous forests burn more frequently among the forest types in this region, as shown by the analysis of forest fire hotspots based on radiation output, fire frequency and fire density [7]. Another example of using statistical data is to analyze the time series characteristics of forest fire distribution in Korea to understand that forest fire occurrence has long-term temporal correlations and to identify areas where the temporal irregularities of forest fire occurrence are consistent with local ones [8].

During wildfires, flame temperatures of up to 1500 K can cause the surface temperature of a pipeline located 10 m from the flames to reach temperatures of 900 K within 15 hours of the fire starting, which can lead to an increase in gas pressure that can result in bursting the pipeline [9]. Martinez et al. [10] performed a series of experiments and obtained ground surface temperatures between 570 K-2175 K during controlled fires and indicating this range of temperature can be observed in actual forest fires. This extreme surface temperature range can be explained by the fact that during forest fires the air temperature can reach values of up to 1600 K. During the thermal radiation heat transfer process, a significant part of the radiant power emitted by flames of up to 290 kW/m^2 is partly absorbed by the ground surface depending on the view (geometry) factor between tree and soil and absorption coefficient of the soil [11]. In an experimental study, similar temperature values, although with lower flux values, were observed as a result of conduction heat transfer occurring through the soil, thus requiring piping to be laid to a minimum allowable depth. Extreme ground temperatures are harmful because the primary cause of failures in gas pipelines is ruptures, especially in aging pipe materials, which require determining a safe installation depth [12].

In addition to the fire risk, other criteria also apply to determining the burial depth. To calculate pipeline burial depth as a function of pipe diameter, lateral earthquake forces may need to be used [13]. Likewise, traffic loads may need to be taken into account when determining the burial depths for different pipe diameters [14]. Another important factor in the severity of forest fires is the energy content, which varies between individual trees, as it determines the duration of burning and thus the peak temperatures that can be achieved during fires. The trees with the highest calorific value include various species of pine. Pine trees have various calorific values, which is released in a fire when the tree is completely burned [15]. For instance Pinus Sylvestris has an average calorific value of 21 MJ/kg. For such a pine tree with a trunk diameter of 27 cm and a height of 25 meters, this value can correspond to a total energy release of 20 GJ. Zeng et al. [16] provides similar figures in their research as 20.8 MJ/for coniferous species in Japan, 19.6–20.5 MJ/kg for 12 tree species grown under a short rotation forestry regime in New Zealand and 17.9–22.9 MJ/kg for indigenous mountain tree and shrub species of the northeastern Himalayan region in India. Burning time is also an important factor as it determines the peak values. Current study assumes that the radiation flux does not decrease over time. However, this is not the case in real fires, as energy release continues to decrease after the heat flux peak as the trees in a given region burn out over time. Temperatures during a wildfire peak sometime after the fire starts and then decline as the fire dies. Therefore, during a forest fire (simulated or real), the soil temperature varies accordingly as a function of time, both at the surface and at different depths in the forest floor [17]. Another factor that, in addition to surface heat flow, determines the intensity of heat diffusion through the soil is soil moisture. According to Preisler et al. [18] when soil is dry, higher temperatures are expected during forest fires due to the effect of humidity on the variation of soil temperature with depth and time. Similarly, another study evaluates the effects of soil water potential and soil water vapor under various soil, fuel, and fire conditions on forest floor temperature and concludes that soil moisture content during fire is crucial in understanding the fire effects on soil properties [19]. As discussed above, vegetation type is a critical factor in the intensity and severity of wildfires. Ground surface temperatures of up to 1260 K have been measured in aspen poplar forest fires, while temperatures in grass and shrub fires are in the range of 675–975 K [20]. In a more recent study, Fajković et al. [21] provides figures in the vicinity of 1350 K found in soil heating during forest fires. In addition to the total energy content, the energy released per unit of time, i.e. the heat release rate (HRR) of burning pine trees in forest fires, is also of crucial importance. However, HRR is greatly influenced by soil moisture content. According to a formula included in the study, a completely dry pine tree has an HRR of 344 kW/kg, while one with 25% moisture has 225 kW/kg, corresponding to a 35% reduction in heat output [22].

Pipelines as a whole, whether gas or general purpose pipelines, must be buried at a safe depth to prevent the risk of wildfires. A recent study examines a modeling method for assessing wildfire heat transfer through the ground to quantify whether the upper limit temperature for general supply operation pressure is exceeded during a wildfire [23]. According to the simulations presented in the study, the model found that the upper limit temperature for the operation pressure of the pipelines was exceeded at depths of up to 0.45 m, which provides a rough "minimum depth of pipeline burial depth" for many applications. Regardless of the cause of the pipe rupture, the most serious consequence of pipe failure is vapor cloud explosions, jet fires, and flash fires. Analysis of one study shows that the rate of serious incidents decreases as pipe diameter and wall thickness increase [24]. Three quarters of the serious incidents occurred in pipelines with relatively thin walls, in fact, a greater wall

thickness could have prevented a large proportion of the incidents. Although increasing the thickness increases pipeline safety, this is often associated with higher material and installation costs. Thus, in addition to a safe burial depth and pipe wall thickness, the pipe material is also important.

The relevant literature mainly deals with aspects of the probability and severity of forest fires as well as the dependence of the consequences of fires on the maximum heat fluxes and the temperatures that occur, and there is only limited work on the time-dependent temperature penetration depth in forest soil. Equally important is the prediction of severity of such fires. Bayat and Yıldız [25] implemented different ML algorithms to forecast burned area size based on various characteristics such as temperature, wind, humidity and precipitation, using records of 512 wildfires that took place in a national park in Northern Portugal.

Analytical Model

The problem at hand is classified as "transient conduction in semi-infinite solids" because the soil surface is exposed to a certain heat flux (radiation) caused by the high temperature of the burning trees above while the heat is propagated throughout the soil. Solutions to this class of problems (transient conduction in semi-infinite solids) can be found in the heat transfer literature, where diagrams or exact analytical expressions such as Eq. (1) [26] and Eq. (2) [27] can be used. These equations apply to the case of constant surface heat flux q_o and constant surface temperature T_s, respectively. However, they do not correspond to the actual situation in a forest fire, as they provide solutions for the case where the surface area is infinite, as shown in Figure 1, while the temperature varies only with depth (z) and time (t). However, in the event of a forest fire, extreme heat flows can occur locally, which leads to heat diffusion not only into the depths but also horizontally on the planes, i.e. in x and y directions, with varying depths.

$$T(z,t) - T_i = \frac{2q_o(\alpha t/\pi)^{1/2}}{k} exp\left(\frac{-z^2}{4\alpha t}\right) - \frac{q_o z}{k} erfc\left(\frac{z}{2\sqrt{\alpha t}}\right) \quad (1)$$

$$\frac{T(z,t)-T_i}{T_i-T_s} = erfc\left(\frac{z}{2\sqrt{\alpha t}}\right) \quad (2)$$

Convection at the surface is neglected because the main mode of heat transfer is radiation, as the magnitude of radiation is much larger. Furthermore, the middle of the forest can be viewed as an enclosure surrounded by trees, where small temperature differences between the ground surface and the surrounding air do not justify the inclusion of convection, which would otherwise have a cooling effect on the ground surface. To illustrate the behavior of soil temperature under constant surface heat flux and constant surface temperature boundary conditions, temperatures for different soil depths are plotted against time using the above equations, as shown in Figure 2. Since the temperature variation becomes negligible below 0.5 m, they are plotted between 0 and 0.4 meters. On the other hand, as can be seen in the constant heat flux graph, temperatures rise indefinitely, suggesting that the constant surface heat flux model is inappropriate. Therefore, a constant surface temperature model is used.

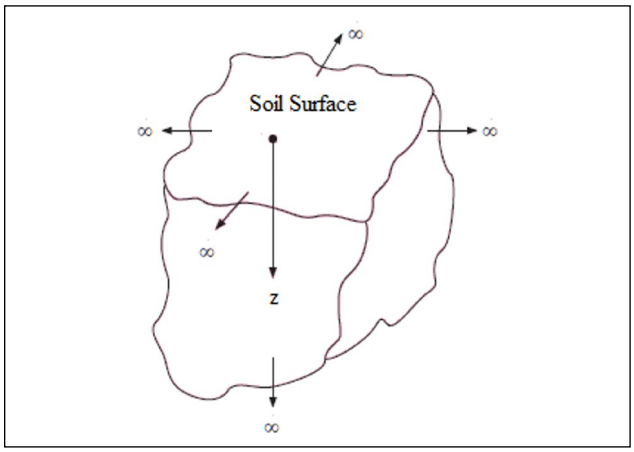

Figure 1. Analytical model (Adapted from Çengel [27]).

Numerical Model

The numerical method is implemented using the Comsol© software package. Analyzing heat transfer by conduction, convection and radiation with the Heat Transfer Module, an add-on product to the COMSOL Multiphysics® simulation platform, makes it possible to find solutions to problems that might otherwise be too complicated to solve analytically. The Heat Transfer Module includes a comprehensive set of features for studying thermal designs and effects of heat loads. For instance, temperature fields and heat flows in components, housings and buildings can be modeled using this module. To virtually examine the real-world behavior of a system or design, multiple physical effects can be easily coupled into one simulation using the multi-physics modeling capabilities included in the software. All functions of the heat transfer module are based on the three types of heat transfer: conduction, convection and radiation. The thermal conductivity of each material can have isotropic or anisotropic thermal conductivity and can be constant or temperature dependent. Convection, the flow of fluids in heat transfer simulations, can be forced or free (natural) convection. Thermal radiation can be accounted for by surface-to-surface radiation or by radiation in semi-transparent media. There are many variations within the types of heat transfer, and the different types must be considered together; in some cases all three at the same time. All of this requires different equations to be processed simultaneously to ensure accurate models.

The first step for the numerical model is to create the geometry for the computational domain. However, due to the fact that during a forest fire there can be localized extreme heat flows, leading to heat diffusion not only to the depth, but also to the surface and to planes parallel to the surface, the problem becomes a three-dimensional problem with $T=f(x,y,z,t)$. The computational domain is 5x5 m at the surface and 1 m at depth. A 3x3 m area is assumed to be exposed to a constant temperature only on the soil surface (Fig. 3) to represent the local radiant energy absorbed by the soil, which is equivalent to the projection area under a burning tree. Selection of the shape of the projected area and the ratio of the projected area to the upper surface of the domain are considered to be unimportant as crown size

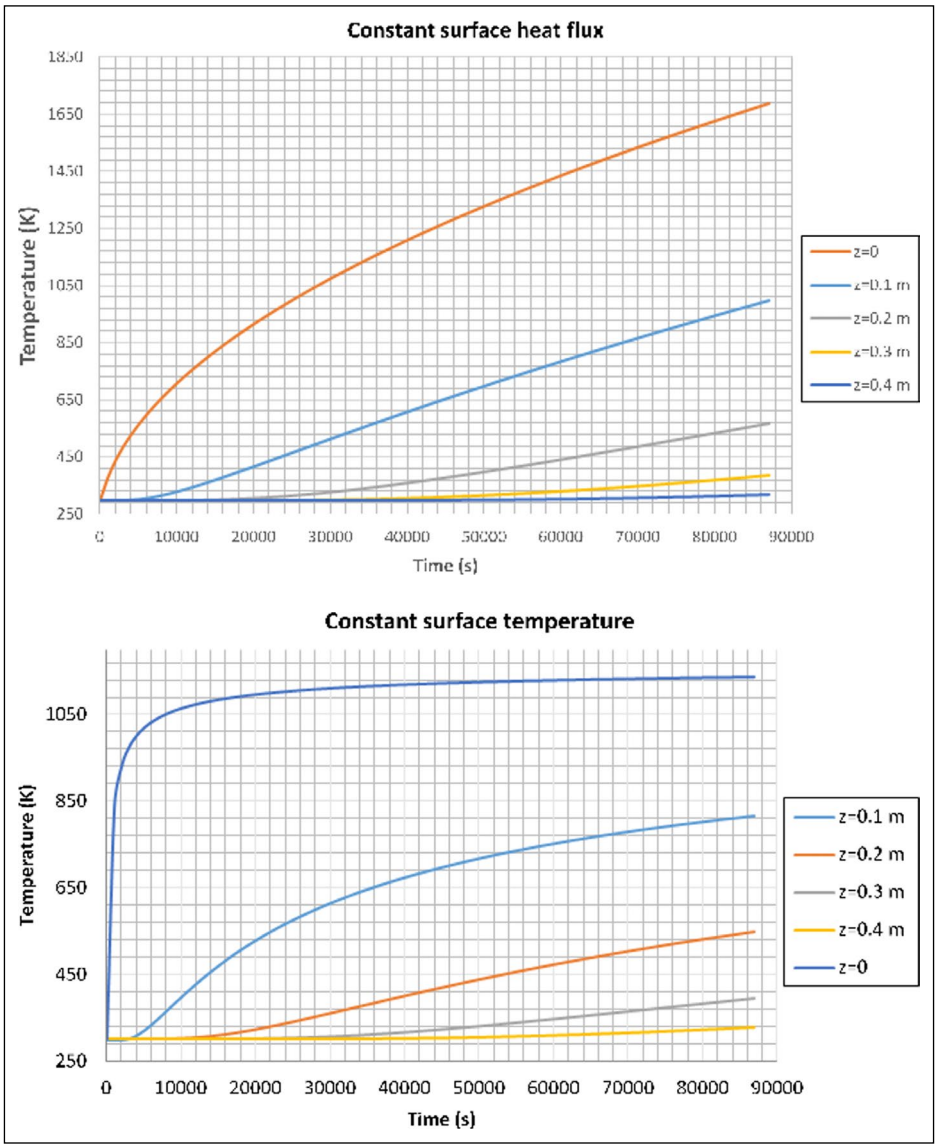

Figure 2. Temperature variation of soil for two different surface boundary conditions.

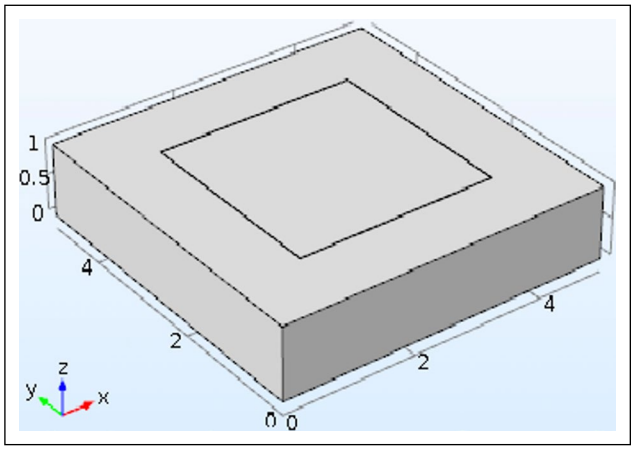

Figure 3. Geometry of the numerical model (5x5 m domain).

and height of trees are highly diversified, therefore an assumption had to be made. It should be noted that the surface of the numerical model has *z=1* m, while the surface in the analytical model has *z=0* m.

The second step is to create a mesh for the computational domain. Mesh size and type, i.e. the number of grid elements, determine the accuracy of the results as well as the execution time and memory usage. The calculations were optimized through a series of trials until the solutions became invariant. "*Physics controlled mesh*" with "*fine mesh*" element size is chosen as the meshing algorithm. *The unstructured mesh structure* in Figure 4 (top) has 152,725 DOFs for the domain shown, the majority of which is *tetrahedral*, plus 58,496 internal DOFs. The middle section of the domain contains much finer elements because temperature gradients are expected to be much higher in this region. To evaluate the grid dependence of the problem at hand, the single tree domain is meshed with an "*extremely fine mesh*" as shown in Figure 4 (below), with the number of mesh elements increased by 24 times and the computation time increased by 4 times, similar to those of "*Fine Mesh*" even though the storage allocation only increased by 30%. On the other hand, when the solutions of two different mesh sizes are compared, one finds that there is no

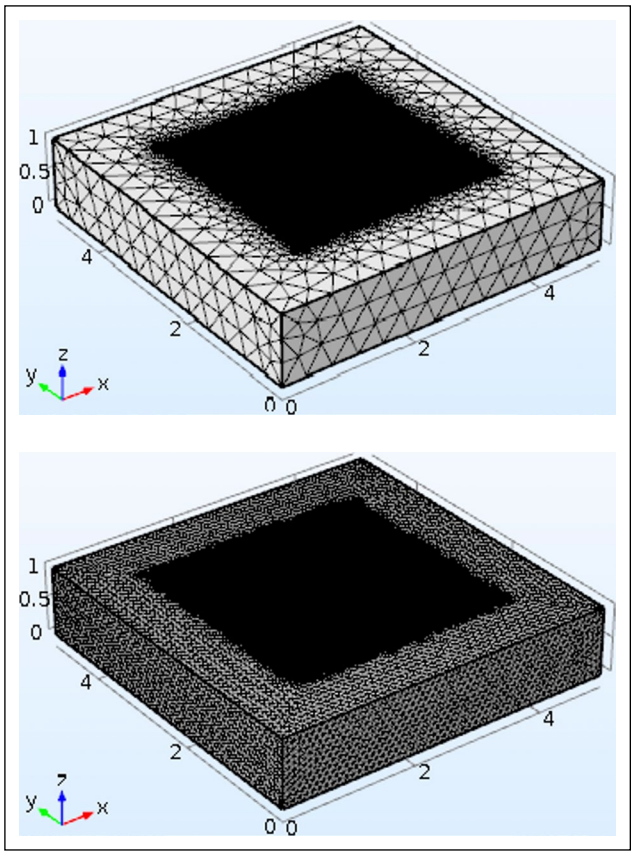

Figure 4. Mesh structures of the model (5x5 m domain). Top: "*Fine Mesh*", Bottom: "*Extremely Fine Mesh*".

noticeable difference, suggesting that the solution is mesh independent, provided the mesh size is fine enough for the problem at hand. Therefore, using a finer mesh than the one used in this work will only result in a waste of computing resources and a much longer running time.

When setting up the model, the software package assumes the following differential equations to solve the transient problem:

$$\rho C_p \frac{\partial T}{\partial t} + \rho C_p \mathbf{u} \cdot \nabla T + \nabla \cdot \mathbf{q} = Q \quad (3)$$

$$\mathbf{q} = -k\nabla T \quad (4)$$

where **u** and **q** are velocity and heat flux vectors, respectively. However, since there is no flow in the domain, **u**=0.

The boundary and initial conditions are 900 °C (for a 3x3 m portion of the domain) and 27 °C (at other locations), respectively. It is assumed that the 3x3 m^2 area is suddenly exposed to the initial condition, which is not the case in an actual fire.

Soil properties are selected from the package's built-in material database. The properties vary with temperature in the numerical solution, while they are usually assumed to be constant in the analytical solution. This is an important feature of the package, apart from the three-dimensionality of the numerical method, as there can be significant variations in properties with temperature: thermal conductivity, specific heat and thermal diffusivity are all piecewise polynomial functions of temperature. As an example, the variation of thermal diffusion coefficient with temperature is

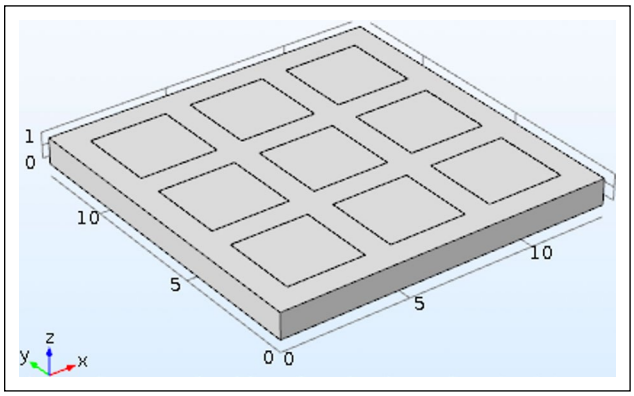

Figure 5. Geometry of the numerical model (16x16 m domain).

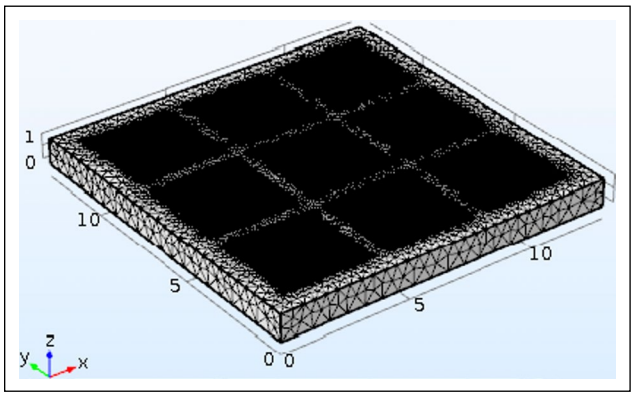

Figure 6. Mesh structure of the model (16x16 m domain).

$$\alpha = 1.81\times10^{-7} - 6.00\times10^{-10}T + 8.89\times10^{-13}T^2 - 4.01\times10^{-16}T^3 \quad (5)$$

Equations 3, 4 and 5 are from the Comsol© documentation published on their website. The density of the soil is assumed to be constant (2000 kg/m^3). It is obvious that the solutions for other types of soil may lead to different results. However, if the data on the thermal properties of the soil is available, the solution can be updated accordingly. As an example, Makarychev and Bolotov [28] provide thermophysical properties of different soil types. According to the authors, depending on the humus content, bulk density of the soil varies between 1320–1380 kg/m^3 while specific heats and thermal conductivities vary between 979-1091 J/kg.K and 0.22–0.388 W/m.K, respectively, corresponding to a thermal diffusivity variation of 1.5×10^{-6}-3×10^{-6} m^2/s. Above equation also provides a similar thermal diffusivity range at a temperature range of 0–150 °C.

To examine the validity of the assumption for the 5x5 m domain, a larger 16x16 m domain accommodating an array of 3x3 trees is also examined, as shown in Figure 5. Figure 6 shows the mesh structure of this larger domain with more than 1,405,906 DOFs plus 495,136 internal DOFs have been solved.

RESULTS AND DISCUSSION

The total computation took 12 minutes for the first setup to converge and 58 minutes for the second setup, when "*Fine Mesh*" grid size is used. The temperatures for the middle of the region (*2.5,2.5,z*) of the first setup, where they are high-

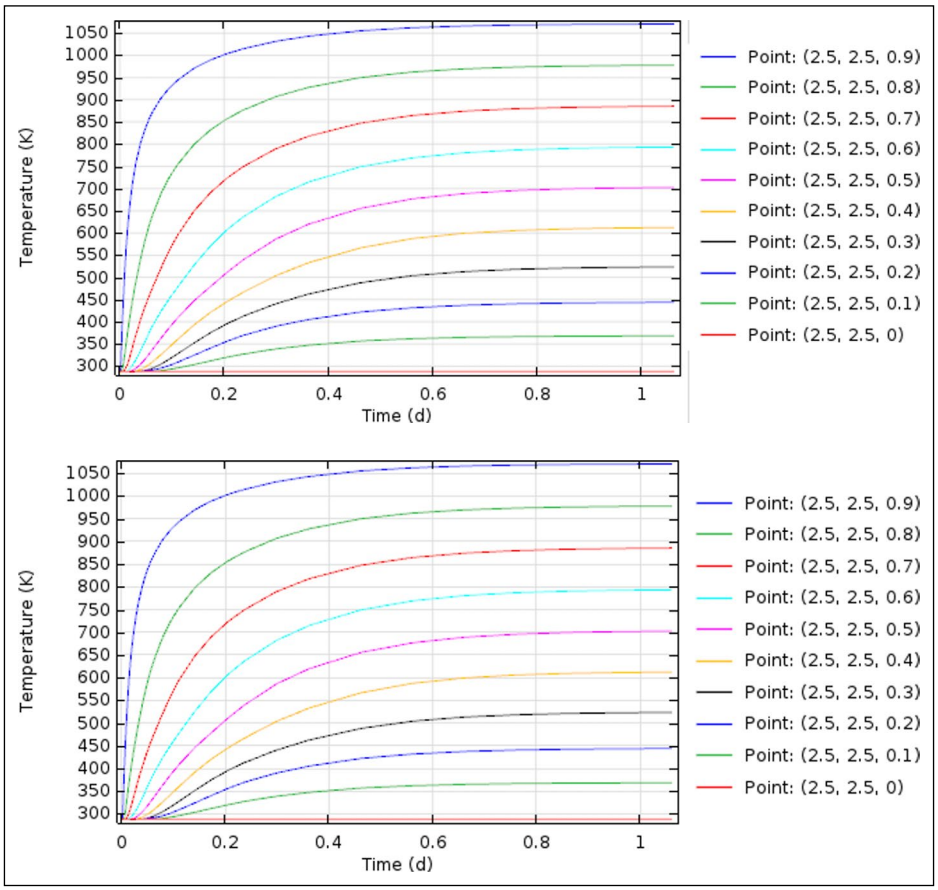

Figure 7. Temperature vs. time for 5x5 m domain. Top: "*Fine Mesh*" Bottom: "*Extremely Fine Mesh*".

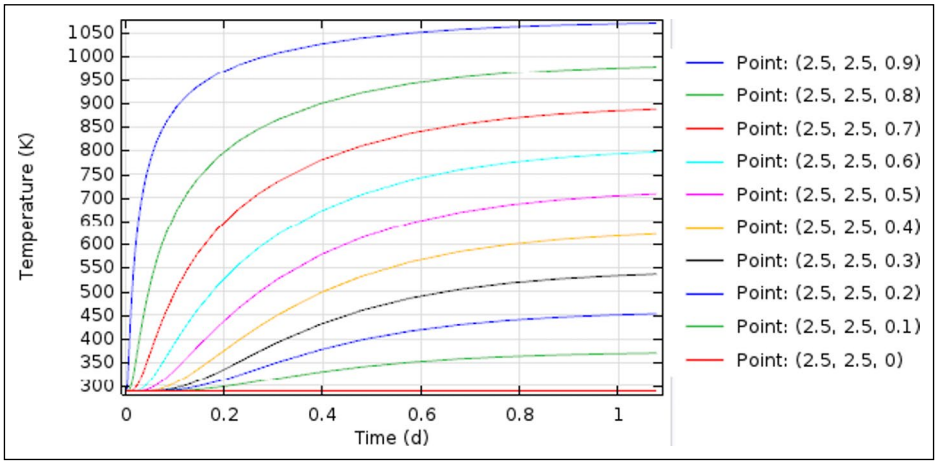

Figure 8. Temperature vs. time for 16x16 m domain.

est at each location parallel to the (*x,y*) plane, are plotted against time as decimal fractions of a day. It should be noted that the surface in the solution corresponds to *z=1 m*, while at the bottom of the domain *z=0 m*. Temperature vs. time for different mesh sizes is shown in Figure 7 (top and bottom), where temperatures peak and level off about halfway through the day. As can be seen from Figure 7, the *Fine Mesh* and *Extremely Fine Mesh* solutions are exactly the same.

These graphs suggest that with the specified soil properties, temperatures at locations deeper than 1 meter are below 300 K and therefore there is no danger to the pipeline. However, even at half depth (*z=0.5 m*), temperatures can be so high that the *pressure* in the gas pipeline can reach a value twice the original value, indicating the possibility of rupture due to increased *hoop stress* as well. The resulting weakening of the pipe material due to increased temperatures leads to a *reduced yield strength*. Petroleum pipelines could also face a similar risk in wildfires, depending on the temperature and thermal expansion of the fluid.

As shown in Figure 8, it is observed that the mean temperatures of the projections of each of the 9 trees in the 16x16 m area are similar to those in the 5x5 m domain. The small

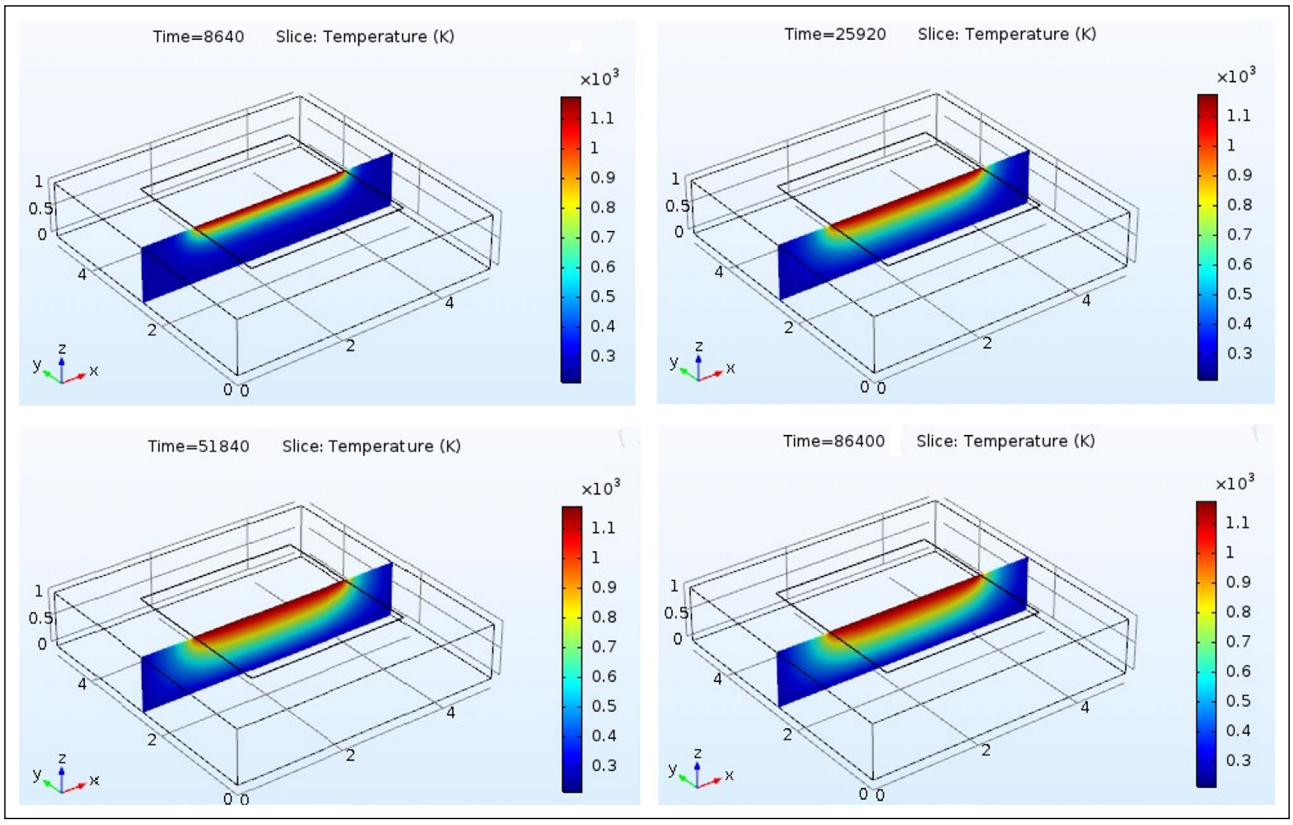

Figure 9. 2-D temperature contour plots on (*x,z*) plane for 5x5 m domain for different times (in seconds) of the day.

differences between the two cases arise from the fact that the single tree domain extends in the x and y directions on horizontal planes (*x,y*) to infinity, where the temperature approaches the initial temperature. On the other hand, the temperature gradients in horizontal planes of the 3x3 tree domain are influenced by the neighboring trees. This is why a 3x3 layout of a given depth takes more time to reach a specific temperature than a single tree, because of the much smaller temperature gradients in *x* and *y* directions, i.e. $^{\partial T}/_{\partial x}$ and $^{\partial T}/_{\partial y}$.

It is also interesting to look at the temperature variation as temperature contours. Figure 9 shows the temperature distribution on a section representing the vertical (*x,z*) plane for different times of the day and Figure 10 in three dimensions at the end of the day.

Both 2D and 3D plots suggest that heat diffuses not only in depth but also in horizontal directions, proving the inappropriateness of the analytical solution given in Equation 1 due to the fact that it is one-dimensional. As shown in Figures 11 and 12, it can be observed that the temperature contours of the projections of each of the 9 trees in the 16x16 m area are also similar to those in the 5x5 m area.

In Figures 9 and 11, it is aimed to provide time dependent temperature distributions in *x* and *z* directions on (*x,z*) plane only as they are same as those in *y* and *z* directions on (*y,z*) plane. On the other hand, time dependent temperature distributions in Figures 10 and 12, temperature distributions are three-dimensional.

The aim of this study is to estimate variations in soil temperature with soil depth due to wildfires, particularly in locations where oil or gas pipelines run in or near forests. The distribution of temperature over soil depth is essential for determining the minimum laying depth of pipes in order to reduce the hazards that may arise from increased surface temperatures of pipes due to heat diffusion through the soil. To prevent catastrophic events, it is important to bury pipelines at a safe depth. Unburied natural gas pipelines can be at great risk due to elevated pipeline surface temperatures during drought-related wildfires due to radiant heat given off by the flames of burning trees. The temperature distributions obtained in this study were compared with those in the publication by Richter et al. [23]. They assume surface heat fluxes of 15–30 kW/m² for wild fires in residential areas. According to their study, at 0.1 m depth, the soil tem-

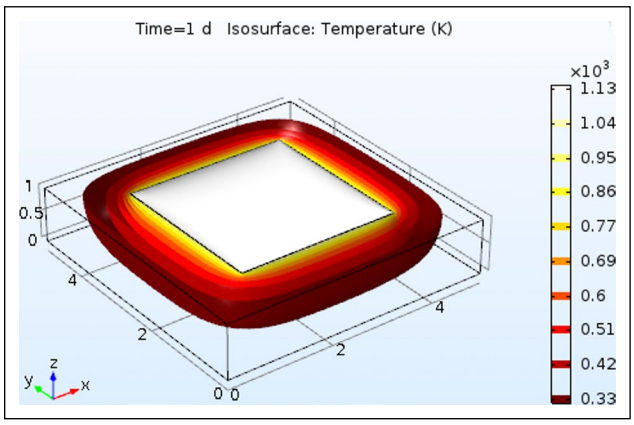

Figure 10. 3-D temperature contour plot for 5x5 m domain (day end).

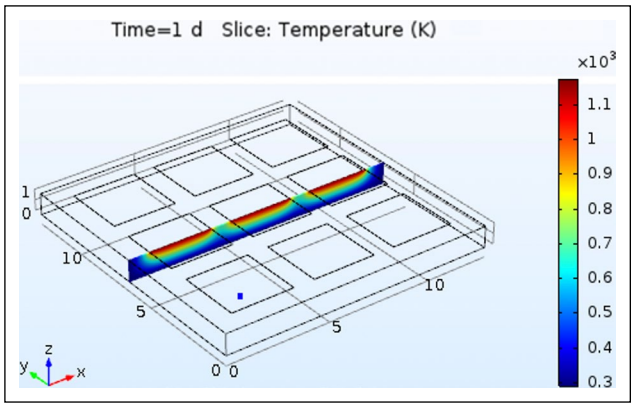

Figure 11. 2-D temperature contour plots on (*x,z*) plane for 16x16 m domain (day end).

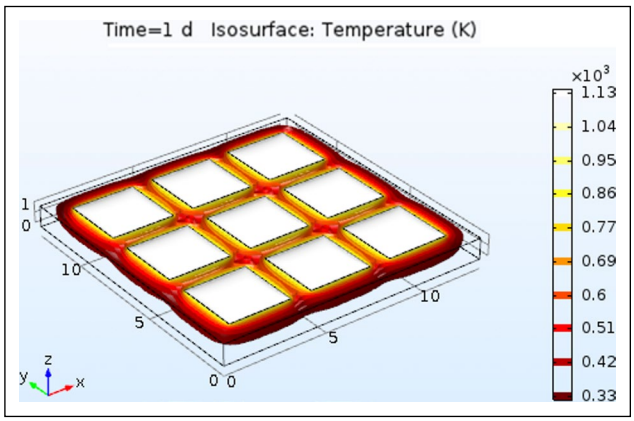

Figure 12. 3-D temperature contour plot for 16x16 m domain (day end).

perature reaches 675 K in 2 hours at 25 kW/m² for which the surface temperature is 2175 K as in this study, while the soil temperature is 700 K at the same depth and time in this study. This small difference between these values of the two studies is attributed to the differences between two analyses: in the work with which this study is compared, a one-dimensional analysis was considered and the soil properties are constant, while in this study, the computational domain is three-dimensional and the soil properties are temperature dependent.

The heat flux value of 25 kW/m² in the case of a tree fire can be justified as follows: assuming a tree crown diameter and trunk height of 3 m and 8 m, respectively, a geometry factor of F_{tg}=0.12 between the tree top and its projection is found using the graph for "View factor between two coaxial parallel disks". Radiation exchange between two surfaces can then be determined as given in Equation 6 [20]:

$$q=\varepsilon F_{tg}\sigma(T_t^4-T_g^4) \quad (6)$$

where ε is emissivity factor, F_{tg} view (geometry) factor between the projection area (circle) of the crown and the ground, σ Stefan-Boltzmann coefficient and T_t and T_g are burning tree and ground temperatures, respectively. Using a rough value of ε=0.85, q can be calculated as 25 kW/m² using burning tree and ground temperatures of 1275 K and 1275 K, respectively, as mentioned in the introduction section.

By closely examining 2D and 3D solutions, the following results were drawn:

1. Under the assumed initial and boundary conditions, soil temperatures tend to level off or reach a quasi-steady state in about half a day, assuming that ground surface temperature boundary conditions remain constant. However, this is not the case in a real fire, as explained in the conclusions section.
2. Since the thermal properties of the soil come from the software's material database, solutions suggest that the minimum laying depth of natural gas or petroleum pipelines is 1 meter to prevent excessive pipe surface temperatures.
3. One-dimensional analytical solutions proposed in the literature are not suitable for this class of problems because the problem at hand is actually three-dimensional.
4. If the data on the thermal properties of the soil is available, it is important to update the solution accordingly, as the solution may give a completely different temperature distribution as a function of space and time.

CONCLUSION

This numerical study investigates spatial and temporal temperature variations in the soil during wildfires. If the site is near a forest or in a forest, the depth of laying the pipeline is particularly important because heat penetration into the ground during forest fires is closely related to one of the soil properties, thermal diffusivity, which can be significantly different in different areas can soil types. It is then important to comprehensively examine the soil properties and determine the laying depth of the pipeline accordingly. Future work could include extensive work considering time-dependent HRR of different species of forest trees during a forest fire. The transient heat released is transferred as convection to the environment above the forest, as radiation to the sky, and also as radiation to the ground beneath the trees. The last part of the released heat is absorbed by the soil, which leads to temporal variations in the soil surface temperature and thus to transient heat conduction in the soil. Apart from the variation in HRR, various tree species have different calorific values when they are completely burned. As a result of this, the rate of radiant energy and the total energy absorbed and stored by the soil during fired will be different. The new study, therefore, aims to provide more realistic temperature distributions in the soil by using tree burn data. However, although conservative, the present study also provides invaluable information in terms of preliminary considerations when selecting gas pipeline locations, as well as calculations of burial depths that take into account extreme temperatures due to wildfires. Another future direction of study could be to conduct a series of experiments with different surface heat fluxes and soil types aimed at measuring the variation of soil temperature with depth and time, although the design of the experimental setup could prove challenging due to physical constraints and power inputs taken into account if realistic results are to be derived from the experimental data.

DATA AVAILABILITY STATEMENT

The author confirm that the data that supports the findings of this study are available within the article. Raw data that support the finding of this study are available from the corresponding author, upon reasonable request.

CONFLICT OF INTEREST

The author declared no potential conflicts of interest with respect to the research, authorship, and/or publication of this article.

USE OF AI FOR WRITING ASSISTANCE

Not declared.

ETHICS

There are no ethical issues with the publication of this manuscript.

REFERENCES

[1] W. Lamb, T. Wiedmann, J. Pongratz, R. Andrew, M. Crippa, J. G. J. Olivier, … and J. Minx, "A review of trends and drivers of greenhouse gas emissions by sector from 1990 to 2018," Environmental Research Letters, Vol. 16, Article 073005, 2021. [CrossRef]

[2] E. Albert-Beldaa, M. B. Hinojosaa, V. A. Laudicinab, and J. M. Moreno, "Soil biogeochemistry and microbial community dynamics in Pinus pinaster Ait. forests subjected to increased fire frequency," Science of the Total Environment, Vol. 858, Article 159912, 2023. [CrossRef]

[3] L. Marfella, R. Marzaioli, and F. A. Rutigliano, "Medium-term effects of wildfire severity on soil physical, chemical and biological properties in Pinus halepensis Mill. woodland (Southern Italy): an opportunity for invasive Acacia saligna colonization?" Forest Ecology and Management, Vol. 542, Article 121010, 2023. [CrossRef]

[4] X. Liu, S. Liang, H. Ma, B. Li, Y. Zhang, Y. Li, … and J. Teng, "Landsat-observed changes in forest cover and attribution analysis over Northern China from 1996–2020," Giscience & Remote Sensing, Vol. 14(1), 2024. [CrossRef]

[5] M. Singh and Z. Huang, "Analysis of forest fire dynamics, distribution and main drivers in the Atlantic forest," Sustainability, Vol. 14, Article 992, 2022. [CrossRef]

[6] H. Heidari, M. Arabi, and T. Warziniack, "Effects of climate change on natural-caused fire activity in Western U.S. national forests," Atmosphere, Vol. 12, Article 981, 2021. [CrossRef]

[7] S. Kumar, and A. Kumar, "Hotspot and trend analysis of forest fires and its relation to climatic factors in the western Himalayas," Natural Hazards, Vol. 114, pp. 3529–3544, 2022. [CrossRef]

[8] T. Kim, S. Hwang, and J. Choi, "Characteristics of spatiotemporal changes in the occurrence of forest fires," Remote Sensing, Vol. 13, Article 4940, 2021. [CrossRef]

[9] A. Basco, A. Di Benedetto, V. Di Sarli, and V. E. Salzano, "How drought is affecting wildfire related risks for natural gas pipeline," in Proceedings of the XXXIX Meeting of the Italian Section of the Combustion Institute, pp. X2.1–X2.6., 2016.

[10] S. I. Martínez, C. P. Contreras, S. E. Acevedo, and C. A. Bonilla, "Unveiling soil temperature reached during a wildfire event using ex-post chemical and hydraulic soil analysis," Journal of Food Engineering, Vol. 90, pp. 20–26, 2009.

[11] B. W. Butler, J. Cohen, D. J. Latham, R. D. Schuette, P. Sopko, K. S. Shannon, D. Jimenez, and L. S, "Measurements of radiant emissive power and temperatures in crown fires," Canadian Journal of Forest Research, Vol. 34, pp. 1577–1587, 2014. [CrossRef]

[12] X. Silvani, F. Morandini, and J. F. Muzy, "Wildfire spread experiments: Fluctuations in thermal measurements," International Communications in Heat and Mass Transfer, Vol. 36, pp. 887–892, 2009. [CrossRef]

[13] A. V. Oskouei, A. Tamjidi, and P. Pourshabani, "Effects of burial depth in the behavior of buried steel pipelines subjected to strike-slip fault," Soil Dynamics and Earthquake Engineering, Vol. 123, pp. 252–264, 2019. [CrossRef]

[14] A. Yiğit, "Embedment depths of natural gas pipelines," El-Cezerî Journal of Science and Engineering, Vol. 8, pp. 471–480, 2021.

[15] R. Petráš, J. Mecko, J. Kukla, and M. Kuklová, "Calorific value of basic fractions of above-ground biomass for Scots pine," Agriculturae Nitriae, Vol. 2, pp. 34–37, 2019. [CrossRef]

[16] W. S. Zeng, S. Z. Tang, and Q. H. Xiao, "Calorific values and ash contents of different parts of Masson pine trees in southern China," Journal of Forestry Research, Vol. 25(4), pp. 779–786, 2014. [CrossRef]

[17] S. S. Sackett, and S. M. Haase, "Measuring soil and tree temperatures during prescribed fires with thermocouple probes," General Technical Reports PSW-GTR-131, Pacific Southwest Research Station, Forest Service, U.S. Department of Agriculture, 1992. [CrossRef]

[18] H. K. Preisler, S. M. Haase, and S. Sackett, "Modeling and risk assessment for soil temperatures beneath prescribed forest fires," Environmental and Ecological Statistics, Vol. 7, pp. 239–254, 2000. [CrossRef]

[19] P. R. Robichaud, W. J. Massman, A. S. Bova, A. G. García, M. Lesiecki, "The Next Generation Soil Heating Model," JFSP Project ID: 15-1-05-11, 2018.

[20] A. W. Bailey and M. L. Anderson, "Fire temperatures in forest communities grass, shrub and Aspen forest communities of Central Alberta," Journal of Range Management, Vol. 33, pp. 37–40, 1980. [CrossRef]

[21] H. Fajković, M. Ivanić, I. Nemet, S. Rončević, Š. Kampić, and D. V. Leontić, "Heat–induced changes in soil properties: fires as cause for remobilization of chemical elements," Journal of Hydrology and Hydromechechanic, Vol. 70(4), pp. 421–431, 2022. [CrossRef]

[22] S. L. Manzello, A. Maranghides, J. R. Shields, W. E. Mell, Y. Hayashi, and D. Nii, "Measurement of firebrand production and heat release rate (HRR) from burning Korean pine trees," International Association for Fire Safety Science (AOFST 7 symposium), 2007.

[23] E. G. Richter, E. C. Fischer, and B. P. Wham, "Simulation of heat transfer through soil for the investigation of wildfire impacts on buried pipelines," Fire Technology, Vol. 58, pp. 1889–1915, 2022. [CrossRef]

[24] H. Wang, and I. J. Duncan, "Likelihood, causes, and consequences of focused leakage and rupture of U.S. natural gas transmission pipelines," Journal of Loss Prevention in the Process Industries, Vol. 30, pp. 177–187, 2014. [CrossRef]

[25] G. Bayat, and K. Yıldız, "Comparison of the Machine Learning Methods to Predict Wildfire Areas," Turkish Journal of Science & Technology, Vol. 17(2), pp. 241–250, 2022. [CrossRef]

[26] T. L. Bergman, A. S. Lavine, and F. Incropera, "Fundamentals of Heat and Mass Transfer, 7th ed., Wiley, pp. 310–317, 2011.

[27] Y. Çengel, "Heat Transfer: A Practical Approach with EES CD," 2nd ed., McGraw Hill, 2002, pp. 228–231.

[28] S. V. Makarychev, and A. G. Bolotov, "Structural-functional concept of thermophysical condition of the soils of Altai Region," Eurasian Journal of Soil Science, Vol. 5(4), pp. 279–284, 2016. [CrossRef]